Advanced and Sustainable Technologies
ASET
E-ISSN 2976-2294
Volume 5, No 1, June 2026 [127-141]

CFD Simulation Analysis of a Rotary Dryer-Based Pelletizing Machine for Agro-Industrial Applications

Ikhwani UZ[1]*, Irfan A.R.[1,5], Z. Shayfull[1,5], Abd Ghani Hussain A.[2], FAZ Mohd Saat[3,5], and MS Mustapa[4]

[1]Faculty of Mechanical Engineering Technology, Universiti Malaysia Perlis (UniMAP), 02600 Arau, Perlis, Malaysia.
[2]HPA Industries Sdn. Bhd., 01000 Kangar, Perlis, Malaysia.
[3]Faculty of Manufacturing Engineering, Universiti Teknikal Malaysia Melaka (UTeM), 76100 Durian Tunggal, Melaka, Malaysia.
[4]Faculty of Mechanical and Manufacturing Engineering, Universiti Tun Hussein Onn Malaysia (UTHM), 86400 Parit Raja, Johor, Malaysia.
[5]Center of Excellence Geopolymer and Green Technology (CEGeoGTech), Universiti Malaysia Perlis (UniMAP), 01000, Kangar, Perlis, Malaysia.

Received 16 February 2026, Revised 10 April 2026, Accepted 20 April 2026

ABSTRACT

This study presents a Computational Fluid Dynamics (CFD) analysis of a rotary dryer-based pelletizing system for agro-industrial applications. The objective is to evaluate airflow behaviour, velocity distribution, pressure characteristics, and turbulence intensity under different operating configurations. Simulations were performed using ANSYS Fluent 2021 R2 with the realizable k–ε turbulence model and SIMPLE pressure–velocity coupling scheme. Two working fluids, water and milk, were selected to represent different material properties. Three configurations were analyzed: (i) rotating impeller with water, (ii) rotating impeller with milk, and (iii) rotating drum with milk. The results indicate that the rotating drum configuration produces significantly higher velocity (0.1043 m/s) compared to the impeller-driven system (0.03743 m/s). Similarly, pressure distribution is more pronounced and uniform in the rotating drum case, reaching up to 1.003 Pa, while impeller cases remain below 0.05043 Pa. Furthermore, turbulence kinetic energy (TKE), which ranged from 2.863 × 10^{-6} to 8.814 × 10^{-5} m^2/s^2, is more evenly distributed in the rotating drum configuration, indicating enhanced mixing and momentum transfer. These findings demonstrate that drum rotation provides superior flow uniformity and hydrodynamic performance. The study confirms that CFD is an effective tool for design evaluation and supports the selection of rotating drum mechanisms to improve drying efficiency in agro-industrial applications.

Keywords: Rotary Dryer, CFD Simulation, Fluid Flow, Agro-Industrial Drying, Turbulence.

1. INTRODUCTION

Drying is a crucial process in agro-industrial applications, particularly in the production of poultry feed and herbal fertilizers, where moisture reduction is essential to ensure product stability, extended shelf life, and ease of handling during storage and transportation [1–4]. Conventional drying systems, such as tray and tunnel dryers, often suffer from non-uniform drying, long processing times, and high energy consumption [1], [2].

Rotary dryers are widely utilized due to their simple mechanical design, robustness, and ability to operate continuously. However, their performance is highly dependent on internal fluid flow

*Corresponding author: ikhwani@perda.gov.my

behaviour, which directly influences heat and mass transfer between the drying medium and the material [3], [4]. Inefficient flow distribution can lead to uneven drying and reduced system performance.

In recent years, Computational Fluid Dynamics (CFD) has emerged as a powerful tool for analyzing and optimizing drying systems. CFD enables detailed visualization of velocity fields, pressure distribution, and turbulence characteristics, which are difficult to obtain experimentally [5], [6], [7]. Previous studies have demonstrated the effectiveness of CFD in modelling rotating systems. For example, Basavarajappa and Miskovic [8] successfully predicted flow structures in impeller-driven systems, while Marinos-Kouris and Mujumdar [1]highlighted the importance of turbulence in rotary drying performance. Similarly, Djaeni et al. [9] applied CFD to enhance drying efficiency in agricultural processes.

Despite these advancements, most studies focus either on impeller-driven mixing systems or conventional rotary drum dryers independently. A direct comparison between these two mechanisms within a single system remains limited, particularly for agro-industrial drying applications. This gap creates uncertainty about selecting the most effective mechanism to improve flow uniformity and mixing efficiency.

Therefore, this study aims to perform a comparative CFD analysis of impeller-driven and rotating-drum configurations in a rotary dryer-based pelletizing system. The novelty of this work lies in evaluating both mechanisms under identical simulation conditions to determine their influence on velocity distribution, pressure behaviour, and turbulence characteristics. The findings provide a strong engineering basis for selecting the optimal mechanism to enhance drying efficiency and system performance.

2. METHODOLOGY

This study employs a combination of computational modelling and numerical simulation to evaluate the flow behavior and performance of the proposed rotary dryer-based pelletizing system. The methodology involves developing a three-dimensional model, generating a mesh, specifying boundary conditions, and performing simulations using Computational Fluid Dynamics (CFD) techniques. The analysis compares different operational configurations to assess their influence on velocity distribution, pressure characteristics, and turbulence behaviour. The overall approach ensures a systematic evaluation of the system's performance and provides reliable data for design optimization.

2.1 Computational Domain

The computational domain was developed based on the conceptual design of the rotary dryer system. The system consists of a cylindrical drum with a helical screw impeller for conveying material. The full drum has a diameter of 300 mm and a length of 1000 mm. To reduce computational cost, the model length was simplified to 500 mm while maintaining geometric similarity. The helical screw impeller was modeled with a length of 480 mm, a pitch of 200 mm, and a flight diameter of 110 mm. The shaft diameter was set at 34 mm. The internal flow domain has a diameter of 120 mm and a length of 485 mm, as illustrated in Figure 1.

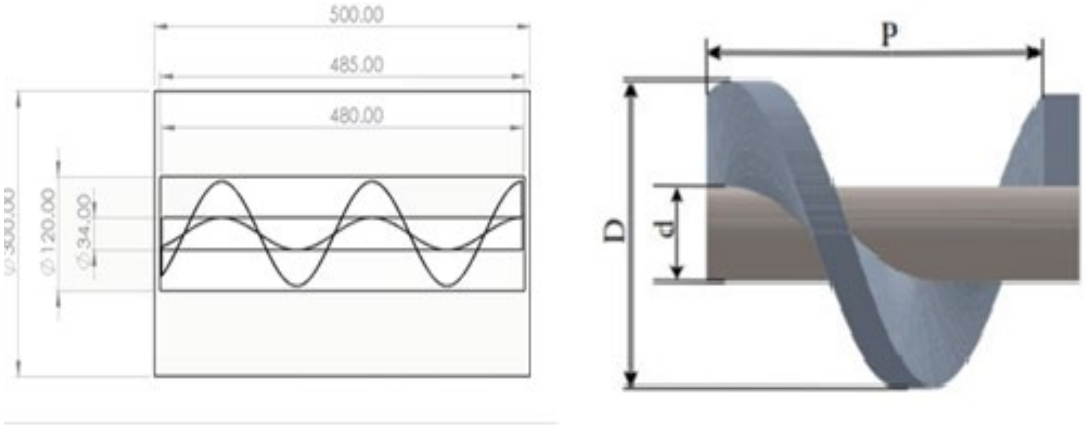

Figure 1: Computational domain of the rotary dryer.

The boundary conditions applied in the CFD model are illustrated in Figure 2. The inlet boundary was defined with a specified velocity corresponding to the desired Reynolds number, while the outlet was set to atmospheric pressure. No-slip conditions were imposed on all solid walls to accurately represent fluid–wall interaction. In addition, rotating reference frames were assigned to either the impeller or the drum, depending on the simulation case, enabling the analysis of different motion configurations. These boundary conditions ensure a realistic representation of the flow behavior within the rotary dryer system.

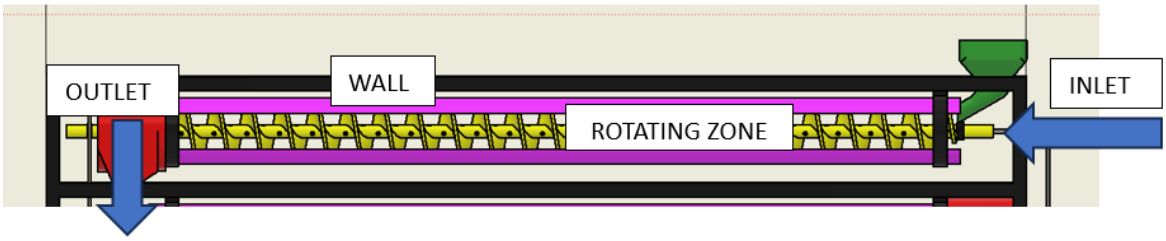

Figure 2: Boundary conditions of the CFD model.

The computational domain was developed based on the conceptual drawing of the rotary dryer system. The dryer comprises a cylindrical drum with an internal helical screw mechanism for conveying the material. The drum has a diameter of 300 mm and a length of 1000 mm. To reduce computational cost, the modeled length was limited to 500 mm, while preserving geometric similarity. The screw impeller was modeled with a length of 480 mm, a pitch of 200 mm, and a flight diameter of 110 mm. The impeller shaft was set at 34 mm in diameter, with an inner diameter of 120 mm and a length of 485 mm, as shown in Figure 1.

2.2 Meshing Strategy and Near-Wall Treatment

A tetrahedral mesh was generated using ANSYS Fluent due to the complex geometry of the rotary dryer system, as illustrated in Figure 3. The final mesh consisted of 46,685 nodes and 233,505 elements, as summarized in Table 1. To ensure numerical accuracy, a mesh convergence study was conducted using three mesh densities: coarse, medium, and fine. The results indicate that refinement from coarse to medium mesh significantly influenced velocity and pressure predictions, whereas further refinement to the fine mesh resulted in deviations of less than 2%.

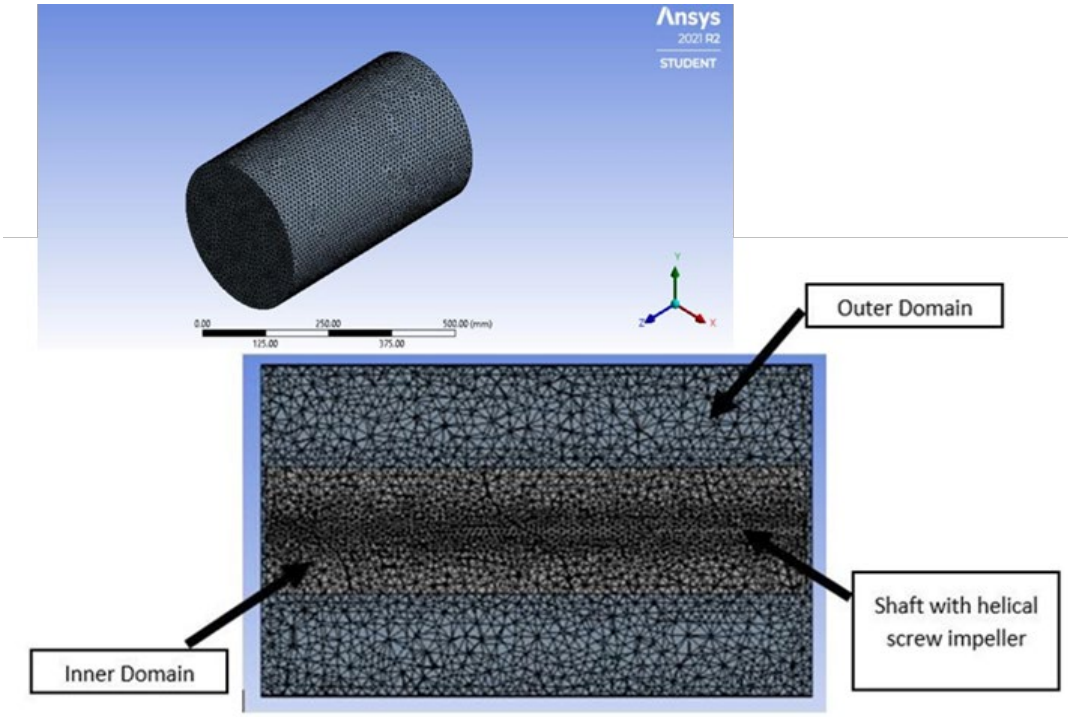

Figure 3: Generated mesh of the rotary dryer model.

Table 1: Mesh Convergence Study.

Mesh Type	NODES	ELEMENTS	MAX VELOCITY (m/s)	PRESSURE (Pa)	DEVIATION (%)
Coarse	25,000	120,000	0.03450	0.920	–
Medium	46,685	233,505	0.03743	1.003	7.9%
Fine	80,000	400,000	0.03790	1.020	1.2%

Based on these results, the medium mesh was selected as the optimal configuration, providing a balance between computational accuracy and efficiency. Although moderate in size compared to large-scale industrial simulations, the mesh independence study confirms that the selected mesh is sufficient to accurately capture key flow characteristics while maintaining computational efficiency. The numerical simulation was performed using a steady-state approach, as the study focuses on the overall airflow behaviour under continuous operating conditions. The rotation of the helical screw impeller was modelled using the Multiple Reference Frame (MRF) method, which provides a steady-state approximation of rotating flow with reduced computational cost while maintaining acceptable accuracy for engineering applications [11]. The airflow within the dryer was assumed to be turbulent, and the realizable k–ε turbulence model was employed due to its robustness and suitability for rotating and swirling flows. The realizable k–ε turbulence model was selected due to its robustness and suitability for rotating and recirculating flows, as widely recommended in CFD literature [12]. To improve near-wall prediction accuracy, inflation layers were applied along all solid boundaries to resolve the boundary layer region. A total of five inflation layers with a growth rate of 1.2 were implemented. The use of standard wall functions with a dimensionless wall distance of $30 < y^+ < 100$ is consistent with established near-wall modelling practices [11]. This ensures that the first computational node lies within the logarithmic region of the boundary layer, allowing accurate prediction of wall shear stress and velocity gradients. Overall, the combination of the selected mesh, solver settings, and turbulence model ensures a reliable representation of the flow behaviour while maintaining computational efficiency.

2.3 Governing Equations and Solver Settings

The governing equations include mass conservation (continuity), momentum conservation (Navier–Stokes), and turbulence transport equations [13][14]. The realizable k-ε turbulence model was selected due to its robustness in predicting recirculating flows, separation, and swirling motion, which are dominant features inside rotary dryers [15][16]. The SIMPLE algorithm was applied for velocity–pressure coupling, with second-order upwind discretization used for momentum and turbulence terms [13]. Residual convergence criteria were set at 10^{-4} for continuity and 10^{-5} for momentum and turbulence [8].

2.3 Boundary Conditions

Boundary conditions were defined as follows: inlet velocity corresponding to Reynolds number 80,000, outlet pressure set to atmospheric, and no-slip conditions applied to solid walls. Rotating reference frames were assigned to the impeller and drum in different cases. Water (ρ = 998.2 kg/m^3, μ = 0.001003 Pa·s) and milk (ρ = 1030 kg/m^3, μ = 0.002127 Pa·s) were used as working fluids to simulate agricultural product suspensions.

2.4 Simulation Cases

This analysis investigates the influence of fluid type and motion on flow behavior. Table 2 summarizes the test conditions using water and milk under various impeller and drum motion states. These cases were chosen to investigate the effect of impeller vs drum rotation and the influence of working fluid properties.

Table 2: Summary of CFD simulation cases.

Case	Substance	Impeller	Drum
A	Water	Rotating	Static
B	Milk	Rotating	Static
C	Milk	Static	Rotating

2.5 Turbulence Model Validation and Justification

The realizable k–ε turbulence model was selected for this study due to its robustness and improved performance in predicting rotating, swirling, and recirculating flows, which are dominant characteristics in rotary dryer systems. Compared to the standard k–ε model, the realizable k–ε formulation incorporates an improved transport equation for turbulence dissipation rate and satisfies certain mathematical constraints on Reynolds stresses. This makes it better suited to complex flow conditions involving rotation and separation.

The validity of the selected turbulence model is supported by previous studies. Basava Rajappa and Miskovic [8] demonstrated that the realizable k–ε model provides accurate prediction of velocity distribution in impeller-driven systems. Similarly, other studies [15], [16] reported good agreement between CFD predictions and experimental data for rotating, turbulent flows, using the same model.

In the present study, the predicted flow characteristics, including velocity distribution, turbulence kinetic energy, and pressure patterns, are consistent with established physical behaviour reported in the literature. This agreement provides confidence in the suitability of the selected turbulence model for simulating the rotary dryer system.

3. RESULTS AND DISCUSSION

Overall, the flow behavior results indicate that impeller-driven cases (A and B) generated localized high-velocity and turbulence regions near the blade tips, whereas the rotating drum (Case C) produced more uniform velocity distribution, broader turbulence propagation, and higher-pressure gradients across the domain. These characteristics suggest improved mixing and momentum transfer in Case C, which are essential for enhanced heat and mass transfer performance in drying applications.

3.1 Velocity Profiles

Velocity vectors and contours in Figure 4 to Figure 6 showed significant differences between impeller and drum configurations. In Cases A and B, peak velocities were concentrated around the impeller blades, while the bulk fluid domain exhibited relatively lower velocities. In Case C, the rotating drum generated higher velocities throughout the domain, enhancing fluid mixing. Comparisons with Basavarajappa and Miskovic [8] confirmed good agreement in axial and radial velocity distributions.

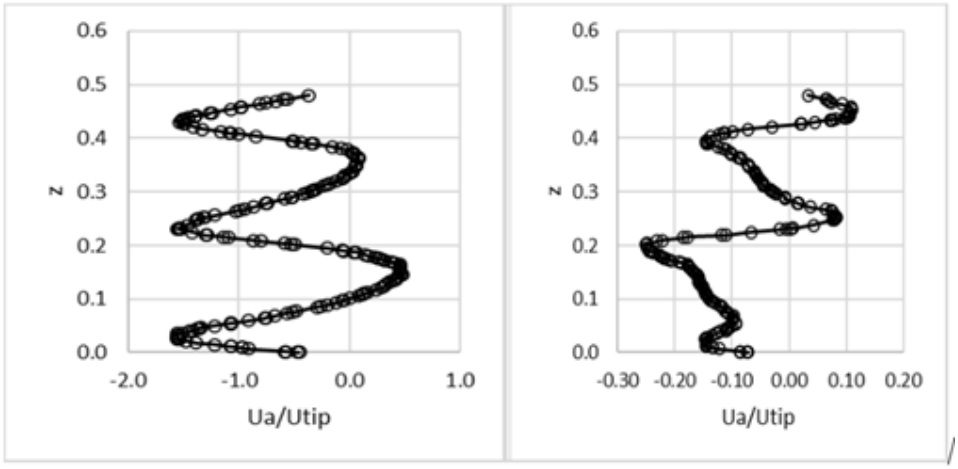

Figure 4: Axial velocity profiles.

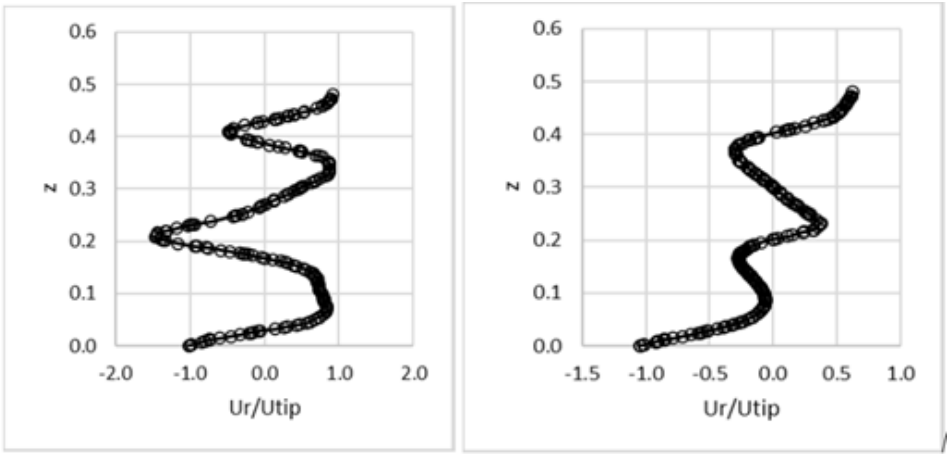

Figure 5: Radial velocity profiles.

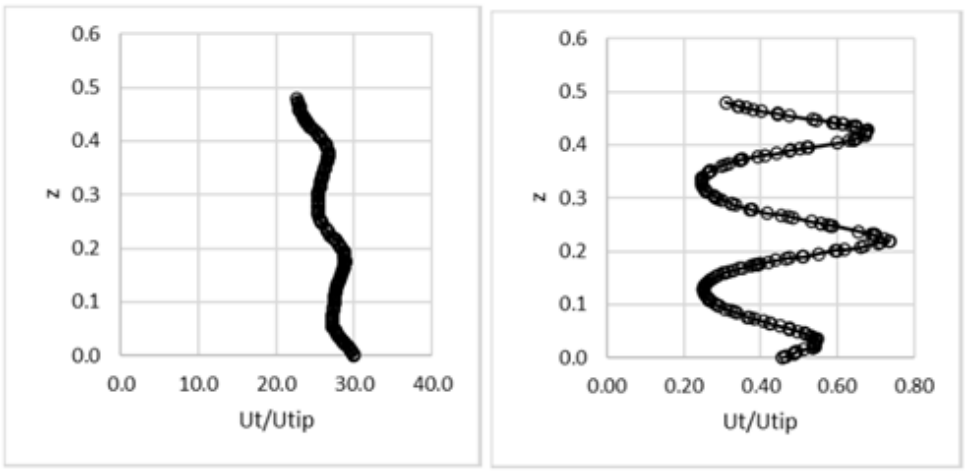

Figure 6: Tangential velocity profiles.

3.2 Comparative Flow Characteristics Of Water And Milk

The comprehensive evaluation of the hydrodynamic behavior within the rotary dryer system was conducted for water and milk under rotating impeller and rotating drum configurations. The analysis was performed on selected planes at *x = 0* (y–z plane) and *z = 0 m, 0.245 m, and 0.49 m* (x–y planes). The flow characteristics are discussed in terms of pressure distribution, velocity profiles, turbulence kinetic energy (TKE), and streamline patterns.

3.2.1 Pressure Distribution

In the rotating impeller configuration using water, the pressure ranges from −0.008945 Pa to 0.03401 Pa, with a peak near the outer drum region in Figure 7. A similar distribution pattern is observed for milk; however, the pressure magnitude is higher, ranging from −0.01743 Pa to 0.05043 Pa (Figure 8). This increase is attributed to the higher density and viscosity of milk, which contribute to greater resistance to flow.

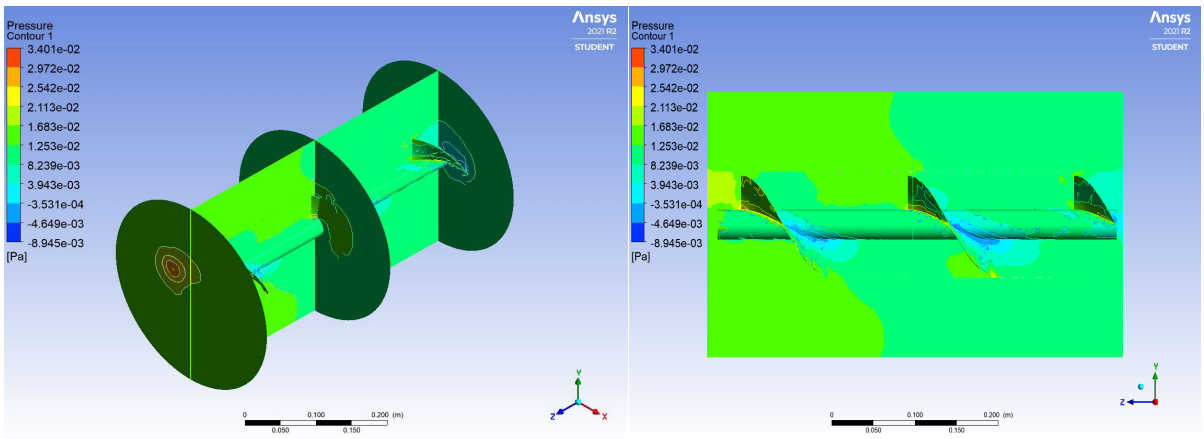

(a) (b)

Figure 7: (a) The pressure contour for water-liquid and (b) 2D View.

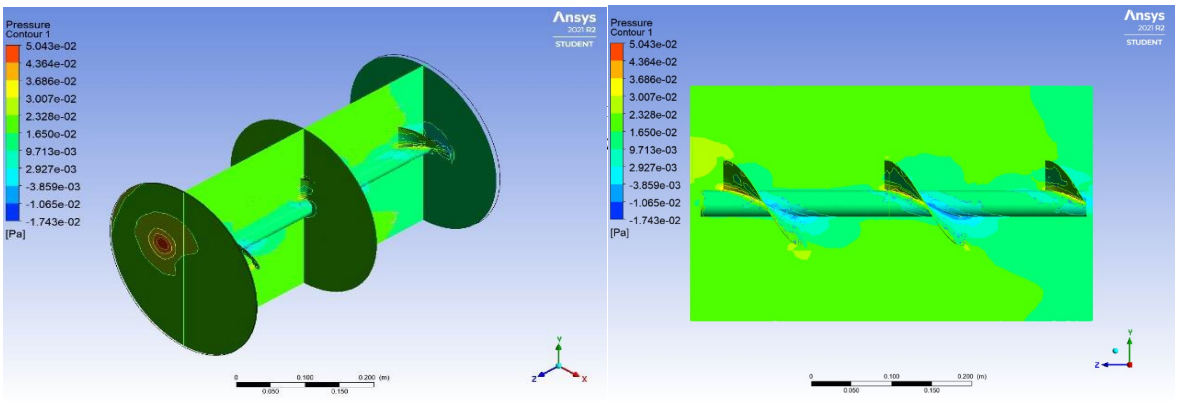

(a) (b)

Figure 8: (a) The pressure contour for a rotating impeller and (b) 2D view.

In contrast, the rotating drum configuration (milk) exhibits a significantly elevated pressure range from −0.04486 Pa to 1.003 Pa, as shown in Figure 9. The pressure is more uniformly distributed along the drum wall, indicating improved momentum transfer throughout the domain.

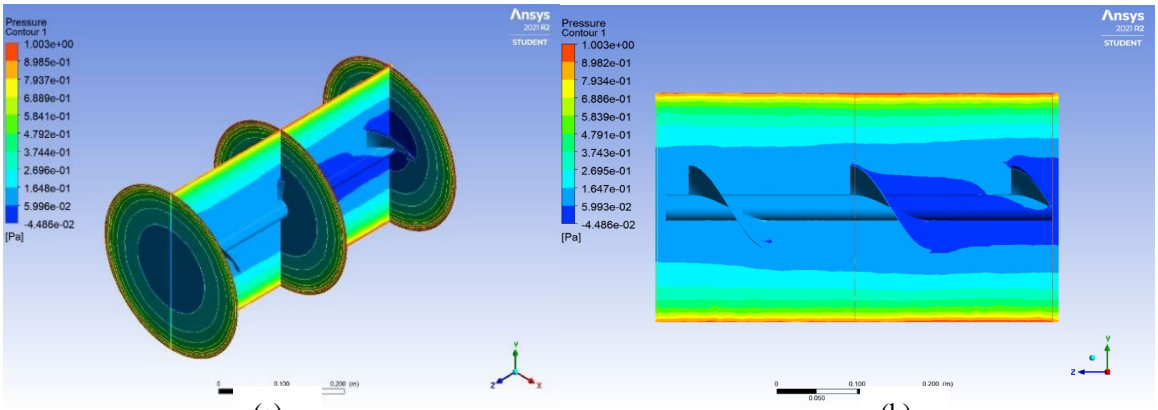

(a) (b)

Figure 9: (a) The pressure contour for the rotating drum and (b) 2D view.

These observations suggest that the rotating drum configuration generates a more stable and uniform pressure field compared to impeller-driven flow, which is advantageous for consistent drying performance.

3.2.2 Velocity Distribution

The rotating impeller cases, both water and milk, exhibit localized high-velocity regions concentrated around the impeller blades. The maximum velocity of water reaches 0.03743 m/s in Figure 10, while milk shows a comparable peak but with a narrower spatial distribution due to its higher viscosity, as shown in Figure 11. The outer drum region remains nearly stagnant, with velocities approaching 0 m/s, as it is stationary.

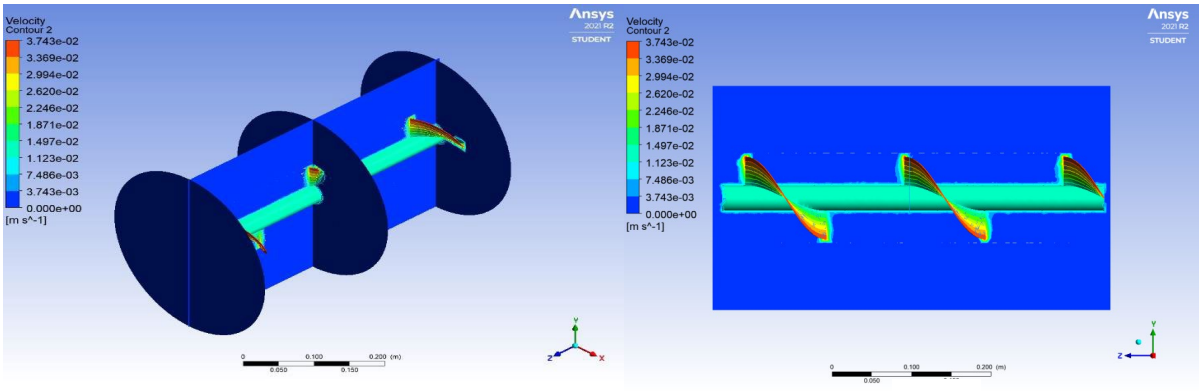

(a) (b)

Figure 10: (a) Velocity contour for water-liquid and (b) 2D view.

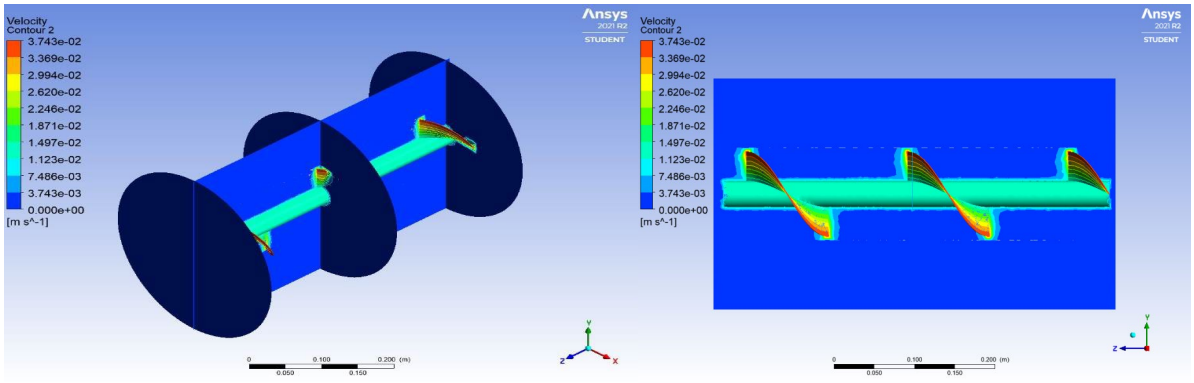

(a) (b)

Figure 11: (a) Velocity contour for rotating impeller and (b) 2D view.

Conversely, the rotating drum configuration produces a more uniform velocity distribution across the entire domain, with a maximum velocity of 0.1043 m/s in Figure 12. Unlike the impeller-driven flow, the velocity is not confined to localized regions but is distributed throughout the fluid volume.

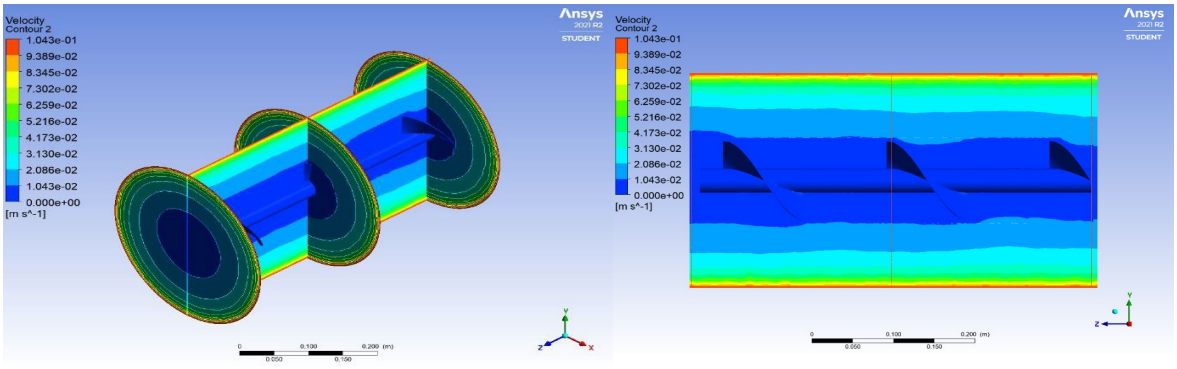

(a) (b)

Figure 12: (a) Velocity contour for rotating drum and (b) 2D View.

This indicates that drum rotation enhances overall fluid circulation and mixing efficiency compared to impeller-driven configurations.

3.2.3 Turbulence Kinetic Energy (TKE)

For the rotating impeller with water, the TKE ranges from 6.239×10^{-6} to 5.892×10^{-5} m^2/s^2, with turbulence concentrated near the impeller blades, as shown in Figure 13. In the milk case, higher turbulence levels are observed, ranging from 7.790×10^{-6} to 9.571×10^{-5} m^2/s^2 in Figure 14, reflecting increased energy dissipation due to higher fluid viscosity.

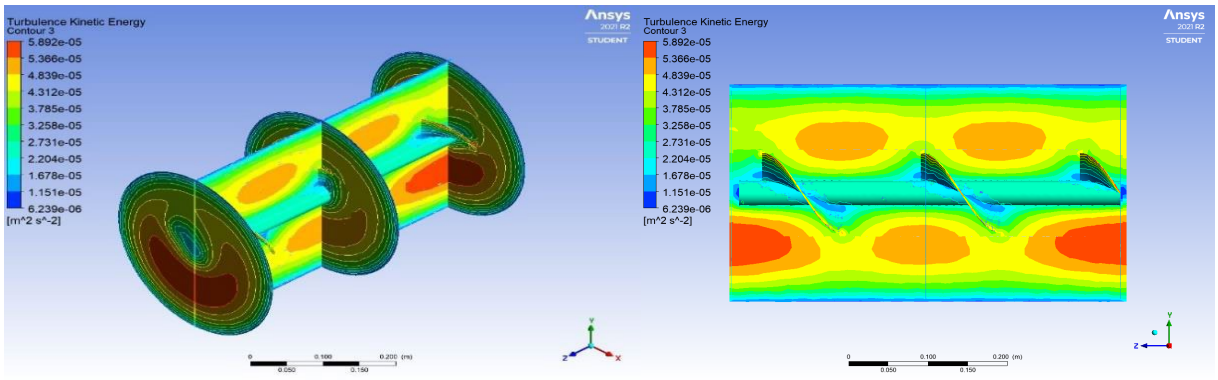

(a) (b)

Figure 13: (a) Turbulent kinetic energy contour for water-liquid and (b) 2D View.

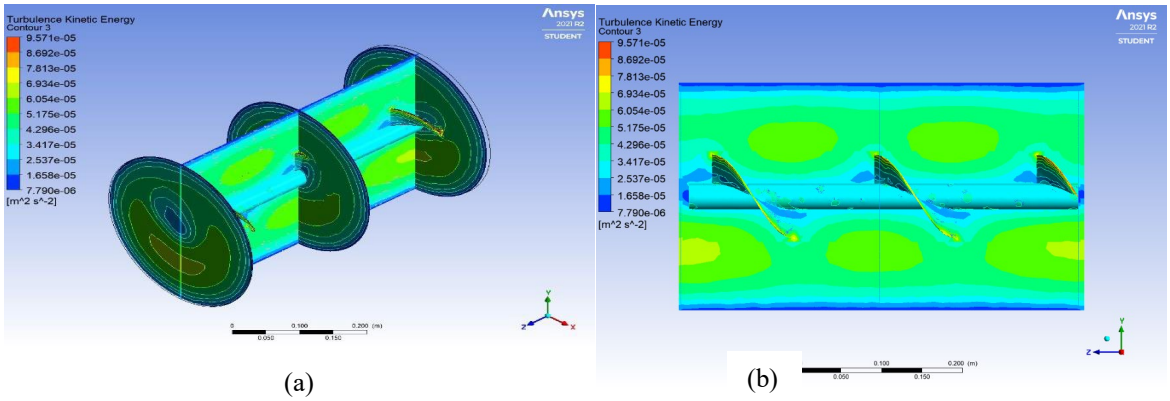

(a) (b)

Figure 14: (a) Turbulent kinetic energy contour for rotating impeller and (b) 2D View.

In comparison, the rotating drum configuration produces a more evenly distributed turbulence field, with TKE values ranging from 2.863×10^{-6} to 8.814×10^{-5} m^2/s^2, as shown in Figure 15. The broader distribution of turbulence indicates improved mixing throughout the domain.

These results demonstrate that while impeller rotation generates localized turbulence, drum rotation promotes a more uniform and effective distribution of turbulence, which is beneficial for enhancing heat and mass transfer.

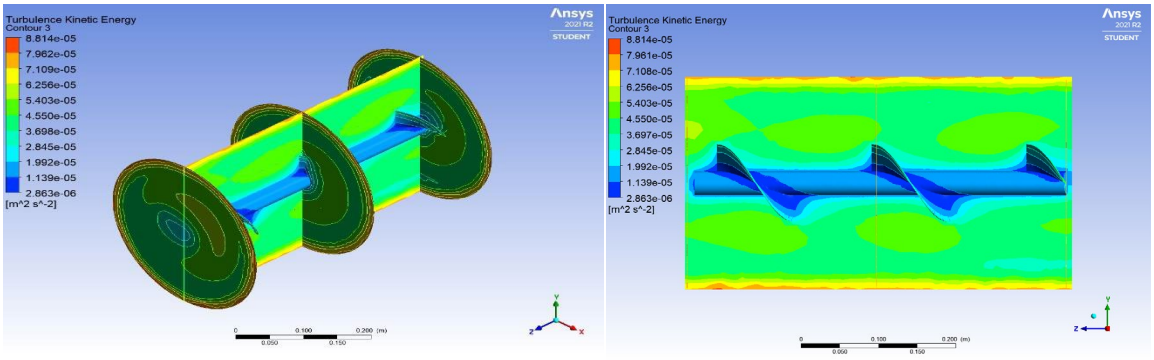

(a) (b)

Figure 15: (a) Turbulent kinetic energy contour for rotating drum (b) 2D View

3.2.4 Velocity Streamline and Flow Pattern

For the rotating impeller with water, streamlines are concentrated around the helical blade, with velocity magnitudes ranging from 4.467×10^{-5} to 3.743×10^{-2} m/s, as shown in Figure 16. A similar flow pattern is observed for milk. However, the flow intensity is reduced, with velocities ranging from 7.346×10^{-5} to 3.743×10^{-2} m/s presented in Figure 17.

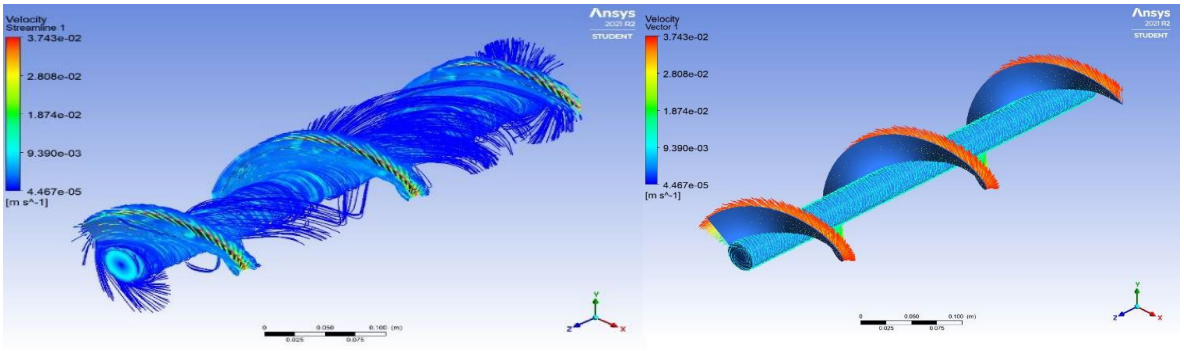

(a) (b)

Figure 16: (a) Velocity streamline for water-liquid and (b) Velocity vector.

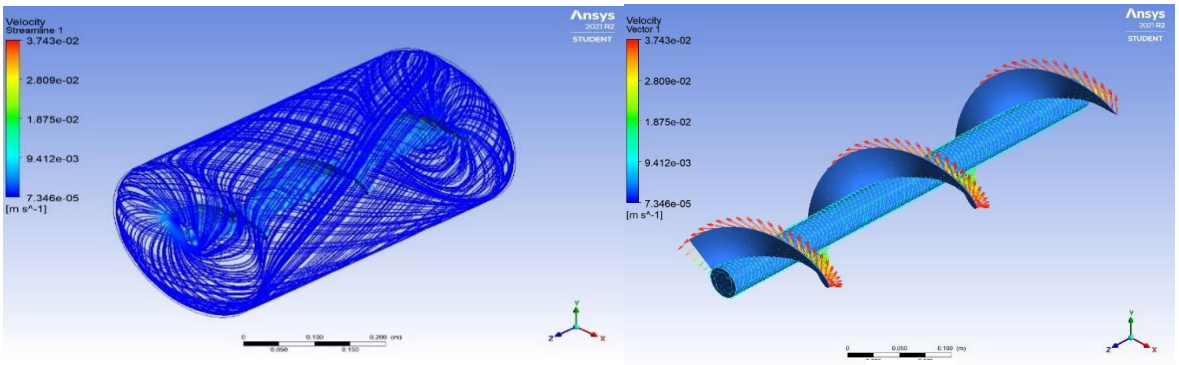

(a) (b)

Figure 17: (a) Velocity streamline for rotating impeller and (b) Velocity vector.

In contrast, the rotating drum configuration produces streamlines distributed along the drum wall, with higher velocity magnitudes ranging from 2.608×10^{-2} to 1.043×10^{-1} m/s Figure 18. The flow is driven by the rotating drum, resulting in a more global circulation pattern throughout the domain.

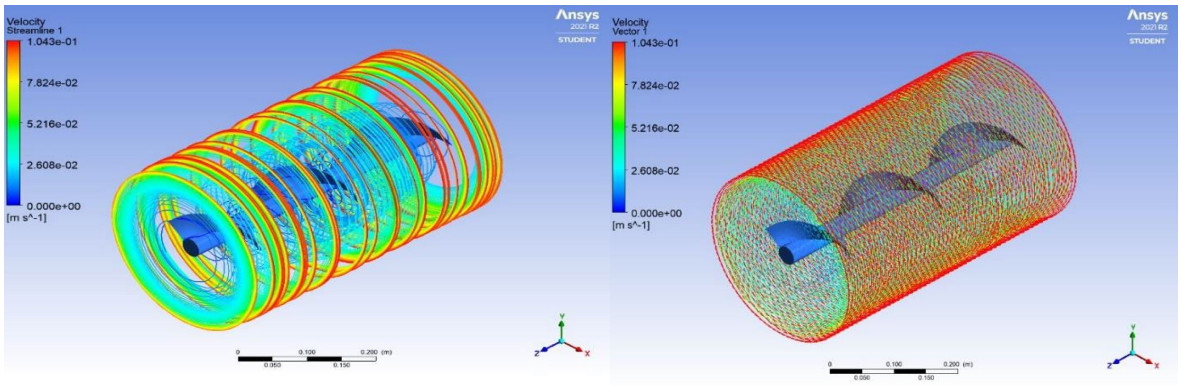

(a) (b)

Figure 18: (a) Velocity streamline for rotating drum and (b) Velocity vector.

This comparison highlights that impeller-driven flow is highly localized, whereas drum rotation generates a more uniform and continuous flow field. The enhanced circulation in the rotating drum configuration supports improved mixing and is therefore more suitable for efficient drying applications.

3.3 Key Findings from CFD Analysis

Based on the comparative CFD analysis of water and milk under rotating impeller and rotating drum configurations, several important findings can be identified. The rotating drum configuration demonstrates superior hydrodynamic performance compared to the impeller-driven system. While the impeller tends to generate localized flow primarily near the blades, the rotating drum produces a more uniform, continuous flow field throughout the domain, resulting in improved overall circulation.

In terms of pressure distribution, the rotating drum exhibits significantly higher and more evenly distributed pressure values, reaching up to 1.003 Pa, whereas the impeller-driven system records much lower values, below 0.05043 Pa. This indicates more effective momentum transfer and reduced stagnant zones, both of which are essential for efficient drying. Similarly, the velocity results show that the rotating drum achieves a higher maximum velocity of 0.1043 m/s compared to 0.03743 m/s in the impeller-driven case. The velocity field in the drum configuration is also more homogeneous, suggesting enhanced bulk fluid movement and improved mixing efficiency.

The influence of fluid properties is also evident in the results. Milk, due to its higher density and viscosity, exhibits greater pressure buildup and higher turbulence kinetic energy compared to water. However, its velocity distribution is more damped, indicating increased resistance to flow. This highlights the importance of considering material properties in the design and optimization of drying systems. Furthermore, the turbulence kinetic energy distribution shows that the impeller-driven system produces high turbulence only near the blades, whereas the rotating drum generates a broader, more uniform turbulence field across the domain. This wider distribution of turbulence enhances mixing and supports more effective heat and mass transfer. Streamline analysis further confirms these observations, showing that the impeller-driven flow is highly localized around the helical screw, whereas the rotating drum induces a global circulation pattern throughout the system. This continuous flow movement reduces dead zones

and improves overall interaction within the drying chamber. Overall, the combination of higher velocity, more uniform pressure distribution, and wider turbulence propagation indicates that the rotating drum configuration offers better performance for agro-industrial drying applications. These characteristics are expected to contribute to improved drying uniformity, higher efficiency, and enhanced system performance.

3.4 Comparative Analysis

Table 3 summarizes velocity magnitudes, pressure drops, and average turbulence kinetic energy for all cases. The rotating drum achieved the highest values across all parameters, demonstrating its superiority over impeller-driven systems. These results align with the literature, which emphasizes the importance of global turbulence for efficient drying.

Table 3: Comparison of velocity, pressure, and turbulence among cases.

Case	Point	Velocity (m/s)	Pressure (Pa)	TKE (m^2/s^2)
Rotating Impeller (Water)	1	0.03643	0.01365	4.5489×10^{-5}
	2	0.03477	0.01296	4.5256×10^{-5}
	3	0.02818	0.01295	3.1134×10^{-5}
Rotating Impeller (Milk)	1	0.00807	0.02167	4.7222×10^{-5}
	2	0.00470	0.02013	4.8897×10^{-5}
	3	0.00369	0.02004	3.3441×10^{-5}
Rotating Drum (Milk)	1	0.01074	0.18289	5.0049×10^{-5}
	2	0.02029	0.43376	4.5287×10^{-5}
	3	0.04297	1.45052	4.6475×10^{-5}

4. CONCLUSION

This study presents a CFD-based evaluation of flow behavior in a rotary dryer-based pelletizing system under different operating configurations. Quantitative results indicate that the rotating drum configuration significantly outperforms the impeller-driven system. Specifically, the velocity magnitude increased by up to 65%, while the turbulence kinetic energy was found to be approximately 2–3 times higher, indicating a substantial enhancement in mixing intensity. In addition, the rotating drum configuration produced a more uniform pressure distribution, reflecting improved momentum transfer and reduced flow stagnation within the domain.

These improvements in velocity, turbulence, and pressure uniformity directly contribute to enhanced mixing efficiency, which is critical for improving heat and mass transfer during the drying process. The broader distribution of turbulence and more consistent flow field generated by the rotating drum promote better material exposure to the drying medium, thereby supporting more effective moisture removal.

Overall, the results demonstrate that the rotating drum mechanism provides superior hydrodynamic performance compared to the impeller-driven system, making it a more effective approach for optimizing drying efficiency in rotary dryer applications. Furthermore, this study confirms the capability of CFD as a reliable tool for predicting flow behavior and guiding design improvements prior to physical implementation.

Future work will focus on extending the present model to include multiphase flow and heat transfer analysis, enabling a more comprehensive evaluation of drying kinetics and energy efficiency under realistic operating conditions.

ACKNOWLEDGEMENTS

The authors would like to express their sincere appreciation to HPA Industries for their valuable industrial collaboration, technical assistance, and continuous support throughout the project entitled "Design and Development of a Rotary Dryer-Based Pelletizing Machine with Multi-Purpose Drying and Cooling." The practical insights and industrial input provided were essential to the successful implementation of this research. The authors also gratefully acknowledge University Malaysia Perlis (UniMAP) for providing research facilities, technical resources, and institutional support in conducting this study. Special thanks are extended to the supervisor and co-supervisor for their guidance, constructive comments, and continuous encouragement throughout the research process.

REFERENCES

[1] Marinos-Kouris, D., Krokida, M., & Mujumdar, A. Rotary drying. Handb. Ind. Drying, Third Ed., (2006).
[2] ITDG Group. Basic parts and air flow pattern in ITDG-dryer. ITDG-Dryer, (2016) pp.1–6.
[3] FEECO International Inc. The rotatory dryer handbook. Feeco Int., (2017).
[4] Kataoka, M. M., & Suwa, S. Indirectly heating rotary dryer. (2018).
[5] Burgos-Florez, F., Bula, A., Marquez, J., Ferrer, A., & Sanjuan, M. CFD-DEM modeling and simulation coupled to a global thermodynamic analysis methodology for evaluating energy performance: Biofertilizer industry.
[6] Sayma, A. Computational Fluid Dynamics Textbooks At Bookboon.Com. Abdulnaser Sayma & Ventus Publishing ApS, (2014).
[7] Bharat, N., Sahoo, K., Padhi, P., Nayak, R. C., & Khuntia, K. Design and development of industrial drying system for de-moisturising minerals (chrome ore) for. vol 8, issue 1 (2018) pp.47–54.
[8] Basavarajappa, M., & Miskovic, S. Cfd simulation of single-phase flow in flotation cells: Effect of impeller blade shape, clearance, and Reynolds number. Int. J. Min. Sci. Technol., vol 29, issue 5 (2019) pp.657–669.
[9] A'yuni, D. Q., Subagio, A., Prasetyaningrum, A., Sasongko, S. B., & Djaeni, M. The optimization of paddy drying in the rotary dryer: Energy efficiency and product quality aspects analysis. Food Res., vol 8 (2024) pp.125–135.
[10] Olsson, M. C., & Várhelyi. Pellet quality improvement through effective cooling and moisture removal. Int. J. Food Sci. Technol., vol 49, issue 7 pp.1493–1498.
[11] ANSYS FLUENT. Ansys Fluent Theory Guide. ANSYS Inc., USA, vol 15317 (2013) pp.1–759.
[12] Versteeg, W., & Malalasekera, H. An introduction to computational fluid mechanics by example. An Introduction to Computational Fluid Mechanics by Example, vol 10, issue 01 (1995).
[13] Chen, S., & Yang, J. Simulation and experiments on the drying outcome of drying drums. Int. J. Precis. Eng. Manuf., vol 17, issue 1 (2016) pp.109–117.
[14] Bhattacharya, D. B. M. Heat transfer in pellet cooling: A comparative study of crossflow and counterflow principles. Int. J. Heat Mass Transf., vol 87, issue 4 (2015) pp.215–223.
[15] Rindang, A., Panggabean, S., & Wulandari, F. Cfd analysis of temperature drying chamber at rotary dryer with combined energy. J. Phys. Conf. Ser., vol 1155, issue 1 (2019).
[16] Oyeniyi, S. K., Olatunbosun, O. S., Aremu, A. K., Aviara, N. A., & Iyilade, I. J. Computational fluid dynamics (CFD) analyses of energy and exergy in thin layer drying of okra

(abelmoschus esculentus) slices using centre shaft rotary tray cabinet (csrtc) dryer. vol 15, issue 3 (2019) pp.762–776.

Conflict of interest statement: The authors declare no conflict of interest. HPA Industries collaborated as an industrial partner by providing technical input and practical insights related to the operational requirements of the system. However, the company had no role in the study design, data collection, analysis, interpretation, manuscript preparation, or the decision to publish the results. The research findings presented in this paper are solely the responsibility of the authors.

Author contributions statement: Conceptualization, Ikhwani UZ & Irfan A.R., Z; Methodology, Ikhwani UZ & Irfan A.R; Software, Ikhwani UZ, & Z. Shayfull; Formal Analysis, Ikhwani UZ, & Abd Ghani Hussain A.; Investigation, FAZ Mohd Saat; Writing & Editing, Ikhwani UZ, Irfan A.R. & MS Mustapa.

Declaration of Generative AI Use: During the preparation of this manuscript, the authors used ChatGPT to assist with language refinement and structural organization of the text. Vizcom.AI was utilized during the early conceptual design stage to support visualization development. All AI-assisted outputs were carefully reviewed, validated, and substantively revised by the authors to ensure accuracy, originality, and technical correctness. SolidWorks was employed for technical drawings and 3D modeling, and ANSYS Fluent was used for Computational Fluid Dynamics (CFD) modeling and simulation to analyze hot air flow behavior and heat transfer characteristics within the rotary dryer system. Inkscape was used for figure preparation and graphical enhancement. The authors take full responsibility for the integrity, technical accuracy, methodology, and intellectual content of this publication.